Supplement of Atmos. Meas. Tech., 14, 7453–7474, 2021
https://doi.org/10.5194/amt-14-7453-2021-supplement

Atmospheric Measurement Techniques
Open Access
EGU

Supplement of

Polarization lidar for detecting dust orientation: system design and calibration

Alexandra Tsekeri et al.

Correspondence to: Alexandra Tsekeri (atsekeri@noa.gr)

S1 Mueller matrices of the atmosphere and of the optical elements of the lidar

S1.1 Backscatter Stokes phase matrices of the atmosphere

S1.1.1 Oriented dust particles

The backscatter Stokes phase matrix of oriented dust particles is shown in Eq. S1

$$\mathbf{F} = \begin{bmatrix} F_{11} & F_{12} & F_{13} & F_{14} \\ F_{12} & F_{22} & F_{23} & F_{24} \\ -F_{13} & -F_{23} & F_{33} & F_{34} \\ F_{14} & F_{24} & -F_{34} & F_{44} \end{bmatrix} = F_{11} \begin{bmatrix} 1 & f_{12} & f_{13} & f_{14} \\ f_{12} & f_{22} & f_{23} & f_{24} \\ -f_{13} & -f_{23} & f_{33} & f_{34} \\ f_{14} & f_{24} & -f_{34} & f_{44} \end{bmatrix} \tag{S1}$$

Where, $f_{ij} = \frac{F_{ij}}{F_{11}}$.

S1.1.2 Atmospheric gases

The backscatter Stokes phase matrix of the gases in the atmosphere is shown in Eq. S2

$$\mathbf{G} = \begin{bmatrix} G_{11} & 0 & 0 & 0 \\ 0 & G_{22} & 0 & 0 \\ 0 & 0 & G_{33} & 0 \\ 0 & 0 & 0 & G_{44} \end{bmatrix} \tag{S2}$$

S1.2 Mueller matrices of the optical elements of the lidar

The Mueller matrices of the optical elements of the lidar are shown in Eq. S3 - S10. The values of the optical element specs are provided by the corresponding manufacturers.

S1.2.1 Receiver optics

(Eq. S.4.12 in Freudenthaler (2016))

$$\mathbf{M_O} = T_O \begin{bmatrix} 1 & D_O & 0 & 0 \\ D_O & 1 & 0 & 0 \\ 0 & 0 & Z_O c_O & Z_O s_O \\ 0 & 0 & -Z_O s_O & Z_O c_O \end{bmatrix} \tag{S3}$$

T_O is the transmittance

D_O is the diattenuation parameter

$Z_O = \sqrt{1 - D_O^2}$

$c_O = cos(\Delta_{T_O})$, $s_O = sin(\Delta_{T_O})$ (Δ_{T_O} is the retardance)

The values provided by the manufacturers are $D_O = 0$, $Z_O = 1$ and $\Delta_{T_O} = 0$

$$\mathbf{M_O} = T_O \begin{bmatrix} 1 & 0 & 0 & 0 \\ 0 & 1 & 0 & 0 \\ 0 & 0 & 1 & 0 \\ 0 & 0 & 0 & 1 \end{bmatrix} \tag{S4}$$

S1.2.2 Half Wave Plate (HWP)

$$\mathbf{M_{HW}}(\theta) = \begin{bmatrix} 1 & 0 & 0 & 0 \\ 0 & c_{4\theta} & s_{4\theta} & 0 \\ 0 & s_{4\theta} & -c_{4\theta} & 0 \\ 0 & 0 & 0 & -1 \end{bmatrix} \tag{S5}$$

θ is the fast-axis-angle relative to the reference plane

$c_{4\theta} = cos(4\theta)$, $s_{4\theta} = sin(4\theta)$

S1.2.3 Quarter Wave Plate (QWP)

$$\mathbf{M_{QW}}(\phi) = \begin{bmatrix} 1 & 0 & 0 & 0 \\ 0 & c_{2\phi}^2 & s_{2\phi}c_{2\phi} & -s_{2\phi} \\ 0 & s_{2\phi}c_{2\phi} & s_{2\phi}^2 & c_{2\phi} \\ 0 & s_{2\phi} & -c_{2\phi} & 0 \end{bmatrix} \tag{S6}$$

ϕ is the fast-axis-angle relative to the reference plane

$c_{2\phi} = cos(2\phi)$, $s_{2\phi} = sin(2\phi)$

S1.2.4 Polarizing Beam Splitter (PBS)

1.2.4.1 Transmitting part

$$\mathbf{M_T} = T_T \begin{bmatrix} 1 & D_T & 0 & 0 \\ D_T & 1 & 0 & 0 \\ 0 & 0 & Z_T & 0 \\ 0 & 0 & 0 & Z_T \end{bmatrix} \tag{S7}$$

$T_T = \frac{T_T^p + T_T^s}{2}$

$D_T = \frac{T_T^p - T_T^s}{T_T^p + T_T^s}$

$Z_T = \sqrt{1 - D_T^2}$

$\Delta_T = 0$

With the use of cleaning polarizing sheet filters after the PBS, considering "ideal cleaning" we get $D_T = 1$ and $Z_T = 0$ (S.10.10 in Freudenthaler (2016)):

$$\mathbf{M_T} = T_T \begin{bmatrix} 1 & 1 & 0 & 0 \\ 1 & 1 & 0 & 0 \\ 0 & 0 & 0 & 0 \\ 0 & 0 & 0 & 0 \end{bmatrix} \tag{S8}$$

1.2.4.2 Reflecting part

$$\mathbf{M_R} = T_R \begin{bmatrix} 1 & D_R & 0 & 0 \\ D_R & 1 & 0 & 0 \\ 0 & 0 & -Z_R & 0 \\ 0 & 0 & 0 & -Z_R \end{bmatrix} \tag{S9}$$

$T_R = \frac{T_R^p + T_R^s}{2}$

$D_R = \frac{T_R^p - T_R^s}{T_R^p + T_R^s}$

$Z_R = \sqrt{1 - D_R^2}$

$\Delta_R = 0$

With the use of cleaning polarizing sheet filters after the PBS, considering "ideal cleaning" we get $D_R = -1$ and $Z_R = 0$ (S.10.10 in Freudenthaler (2016)):

$$\mathbf{M_R} = T_R \begin{bmatrix} 1 & -1 & 0 & 0 \\ -1 & 1 & 0 & 0 \\ 0 & 0 & 0 & 0 \\ 0 & 0 & 0 & 0 \end{bmatrix} \tag{S10}$$

S2 Calculation of the measured signals $\mathbf{I_{i\_k\_s}}$

The measured signals $I_{i\_k\_s}$ for laser $i = LA$, LB, at the detection unit after telescope $k = TA$, TB, at the detector $s = T$, R ("Transmitted" and "Reflected" channel after the PBS_k, respectively), are shown in Eq. S11, S12 and S13. In Eq. S11-S13 we consider background-corrected values and we omit the electronic noise at the detectors.

$$I_{i\_k\_s} = \eta_{s\_k} \boldsymbol{M}_{i\_k} (\mathbf{F} + \mathbf{G}) \boldsymbol{i}_i \tag{S11}$$

$$\boldsymbol{M}_{i\_TA} = E_{i\_TA} \boldsymbol{e} \mathbf{M}_{s\_TA} \mathbf{M}_{O\_TA} \tag{S12}$$

$$\boldsymbol{M}_{i\_TB} = E_{i\_TB} \boldsymbol{e} \mathbf{M}_{s\_TB} \mathbf{M}_{QW\_TB} \mathbf{M}_{O\_TB} \tag{S13}$$

In Eq. S11, η_{s_k} is the amplification of the signals of the lasers at $s = T$ or R detector of the detection unit after telescope k, $\boldsymbol{M}_{i\_k}$ is a row vector expressing the measured polarization at the detection unit after telescope k, $\mathbf{F}$ (Eq. S1) and $\mathbf{G}$ (Eq. S2) are the backscatter Stokes phase matrices of the dust particles and of the gas molecules, respectively, at a certain range in the atmosphere, and $\boldsymbol{i}_i$ is the Stokes vector of the light from the emission unit of laser i (Eq. S14 and S15). Equations S12 and S13 describe in more detail the vectors $\boldsymbol{M}_{i\_k}$: $E_{i\_k} = A_k O_{i\_k} T(0,r)^{-2} E_{oi}$, where A_k is the area of the telescope k, O_{i_k} is the overlap function of the laser beam receiver field-of-view with range 0-1 (for laser i and telescope k), $T(0,r)$ is the transmission of the atmosphere between the lidar at range $r = 0$ and a specific range in the atmosphere, and E_{oi} is the pulse energy of laser i. $\boldsymbol{e} = [1,0,0,0]$ denotes the measurement of only the intensity of light reaching the APDs. $\mathbf{M}_{s\_k}$ is the Mueller matrix of the PBS_k followed by cleaning polarizing sheet filters (Eq. S8 and S10), $\mathbf{M}_{O\_k}$ is the Mueller matrix of the receiver optics (i.e. telescope k, collimating lenses, bandpass filter; Eq. S4), and $\mathbf{M}_{QW\_TB}$ is the Mueller matrix of the QWP_{TB} (Eq. S6).

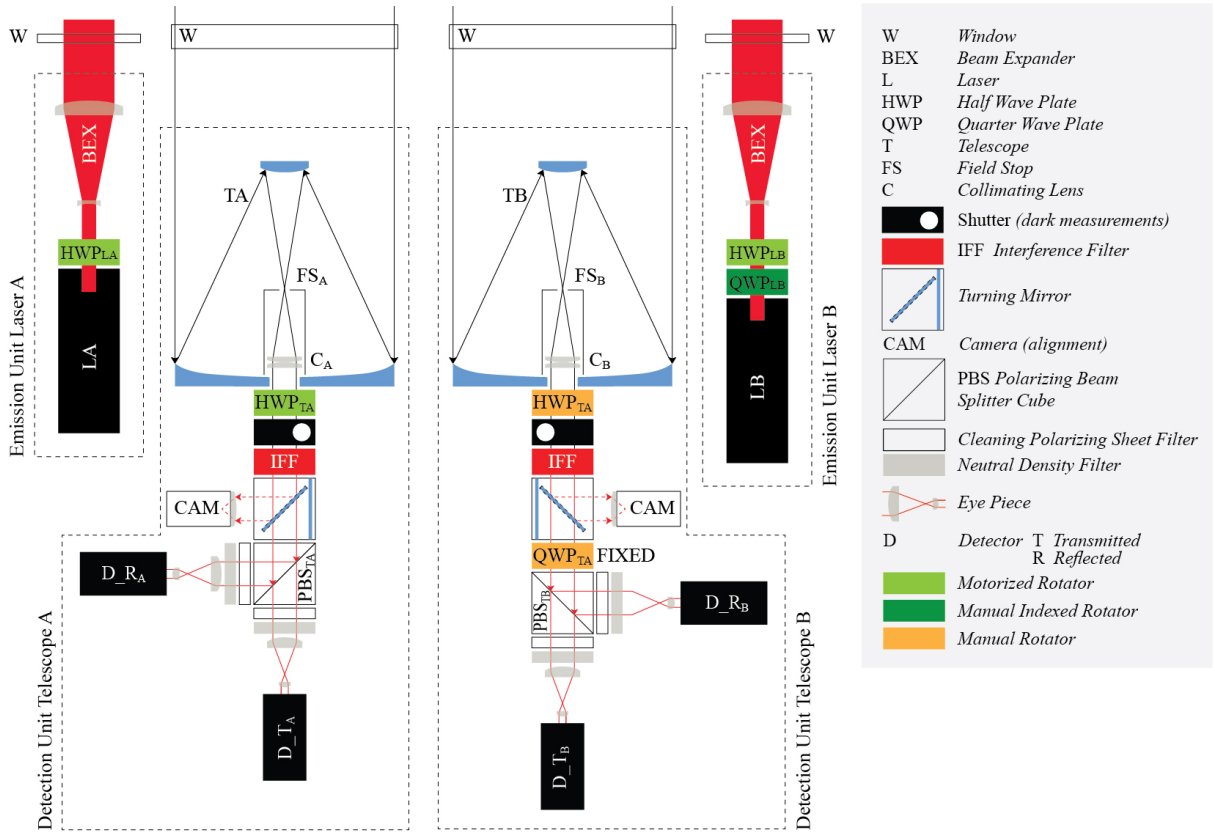

Figure S1: Sketch of the emission and detection units of the system: two lasers shooting alternatively (LA and LB), with the backscattered signals correspondingly alternatively collected by two telescopes (TA and TB) and then redirected at two detectors for each telescope (D_s, $s = T, R$ as of "Transmitted" and "Reflected" channels). The polarization of the light emitted from each laser is changed appropriately, using the Half Wave Plate HWP_{LA} for laser A and the Quarter Wave Plate QWP_{LB} followed by the HWP_{LB} for laser B. The laser beam of each laser is expanded with a beam expander (BEX). At the detection unit after the first telescope the light goes through PBS_{TA} and after the second telescope the light goes through QWP_{TB} and PBS_{TB}. The HWP_{TA} at telescope A is used to correct the rotation of the PBS_{TA} (Section 4.1 in the manuscript). The HWP_{TB} at telescope B is used to check the position of the QWP_{TB} with respect to the PBS_{TB} (Section S4). The shutter at each telescope is used for performing dark measurements. The camera at each telescope is used for the alignment of the laser beams with the field-of-view of the telescope.

S2.1 The polarization of the light from the emission units of lasers A and B

The Stokes vector of the light from the emission units of laser A and B is defined with respect to the "frame coordinate system", shown in Fig. S2a, and is provided by $\boldsymbol{i}_{LA}$ (Eq. S14) and $\boldsymbol{i}_{LB}$ (Eq. S15), respectively. The light emitted directly from the lasers ($\boldsymbol{i}_{lsr\_LA}$ and $\boldsymbol{i}_{lsr\_LB}$) is considered to be 100% linearly-polarized, with angle of polarization ellipse with respect to the frame coordinate system α_{LA} and α_{LB} for lasers A and B, respectively. The polarization of the light from the whole emission unit is then defined according to the position of the optical elements in front of the laser, i.e. the HWP_{LA} in front of laser A, and the QWP_{LB} followed by

the HWP_{LB} in front of laser B (Fig. S1, Fig. S2d and e; Eq. S14 and S15). We use the angles $\vartheta_{LA} = \theta_{LA} - \frac{\alpha_{LA}}{2}$ and $\varphi_{LB} = \phi_{LB} - \alpha_{LB}$ to simplify Eq. S14 and S15. As described in Section 4 in the manuscript, $\vartheta_{LA} = 22.5^o$, $\varphi_{LB} = -30^o$, $\phi_{LB} = \alpha_{LB} - 30^o$ and $\theta_{LB} = \frac{\alpha_{LB}}{2} - 12.2^o$.

$$\boldsymbol{i}_{LA} = \mathbf{M}_{HW\_LA}(\theta_{LA})\boldsymbol{i}_{lsr\_LA}(\alpha_{LA}) = \begin{bmatrix} 1 \\ c_{(4\theta_{LA}-2\alpha_{LA})} \\ s_{(4\theta_{LA}-2\alpha_{LA})} \\ 0 \end{bmatrix} = \begin{bmatrix} 1 \\ c_{4\vartheta_{LA}} \\ s_{4\vartheta_{LA}} \\ 0 \end{bmatrix} = \begin{bmatrix} 1 \\ 0 \\ 1 \\ 0 \end{bmatrix} \tag{S14}$$

$$\begin{aligned} \boldsymbol{i}_{LB} = \mathbf{M}_{HW\_LB}(\theta_{LB})\mathbf{M}_{QW\_LB}(\phi_{LB})\boldsymbol{i}_{lsr\_LB}(\alpha_{LB}) = \begin{bmatrix} 1 \\ c_{2(\phi_{LB}-\alpha_{LB})}c_{(4\theta_{LB}-2\phi_{LB})} \\ c_{2(\phi_{LB}-\alpha_{LB})}s_{(4\theta_{LB}-2\phi_{LB})} \\ -s_{2(\phi_{LB}-\alpha_{LB})} \end{bmatrix} = \\ = \begin{bmatrix} 1 \\ c_{2\varphi_{LB}}c_{(4\theta_{LB}-2\phi_{LB})} \\ c_{2\varphi_{LB}}s_{(4\theta_{LB}-2\phi_{LB})} \\ -s_{2\varphi_{LB}} \end{bmatrix} = \begin{bmatrix} 1 \\ 0.85 \\ 0.17 \\ 0.5 \end{bmatrix} \end{aligned} \tag{S15}$$

The "DU_{TA} coordinate system" and the "DU_{TB} coordinate system" in Fig. S2b and c are the right-handed coordinate systems of the detection units after telescopes A and B, respectively. The $x_{DU_{TA}}$ and $y_{DU_{TA}}$ axis coincide with the incidence plane of PBS_{TA}, and the $x_{DU_{TB}}$ and $y_{DU_{TB}}$ axis coincide with the incidence plane of PBS_{TB}. The optical elements are considered to be well aligned with eachother in the detection units (because their holders are manufactured and assembled in a mechanical workshop with high accuracy), but the detection units are possibly rotated around the optical axis with respect to the frame coordinate system by angles ω_{TA} and ω_{TB}, respectively (Fig. S2b and c). The Stokes vectors of the light collected at telescope A and B are consequently described including a multiplication with the rotation matrices $\mathbf{R_{TA}}(-\omega_{TA})$ and $\mathbf{R_{TB}}(-\omega_{TB})$, respectively (see Eq. S.5.1.7 in Freudenthaler˙2016). This rotation affects the measurements of the polarized components after PBS_{TA}, but not after PBS_{TB}. The rotation of the detection unit after telescope A is corrected using the HWP_{TA}, as shown in Section 4.1 in the manuscript.

Sections S2.2, S2.3, S2.4 and S2.5 provide the analytical calculations for the formulas of $I_{i\_k\_s}$, taking into account all the optical elements of the system, including their misalignments.

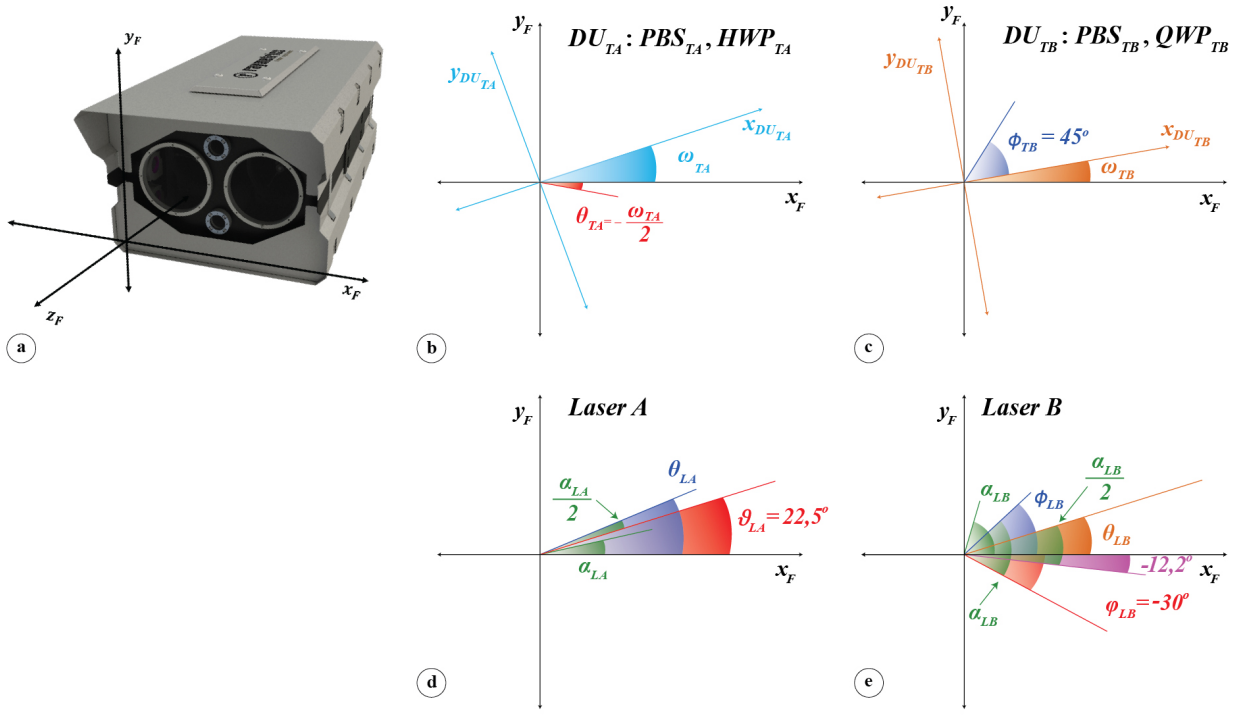

Figure S2: a) The "frame coordinate system" (black) is the reference coordinate system with x_F-axis parallel to the horizon. b) The "DU_{TA} coordinate system" (light blue) is the coordinate system of the detection unit after telescope A, which is rotated with respect to the frame coordinate system by an angle ω_{TA}. The effect of this rotation on the signals is corrected using HWP_{TA}, placed at $\theta_{TA} = -\frac{\omega_{TA}}{2}$ (red) with respect to the x_F-axis. c) The "DU_{TB} coordinate system" (orange) is the coordinate system of the detection unit after telescope B, which is rotated with respect to the frame coordinate system by an angle ω_{TB} . The rotation does not affect the measured signals. The QWP_{TB} before PBS_{TB}, is placed at $\phi_{TB} = 45^o$ with respect to the $x_{DU_{TB}}$-axis. d) The light emitted directly from laser A is linearly-polarized with unknown angle of polarization α_{LA}. As shown in Eq. S14, using the HWP_{LA} with fast-axis-angle $\theta_{LA} = 22.5^o + \frac{\alpha_{LA}}{2}$, we produce the light emitted from the emission unit of laser A with angle of polarization $2\vartheta_{LA} = 45^o$. e) The light emitted directly from laser B is linearly-polarized with unknown angle of polarization α_{LB}. As shown in Eq. S15, using the QWP_{LB} with with fast-axis-angle $\phi_{LB} = \alpha_{LB} - 30^o$, and the HWP_{LB} with fast-axis-angle $\theta_{LB} = \frac{\alpha_{LB}}{2} - 12.2^o$, we produce the elliptically-polarized light emitted from the emission unit of laser B with angle of polarization 5.6^o and degree of linear polarization 0.866.

S2.2 $\mathbf{I_{LA\_TA\_s}}$: The signals from laser A, at the detection unit after telescope A

The measurements of the backscatterred light of laser A at the detectors of telescope A are provided in Eq. S16. The rotation of the detection unit after telescope A by an angle ω_{TA} (Fig. S2b) is taken into account using the rotation matrix $\mathbf{R}_{TA}(-\omega_{TA})$. The HWP_{TA} (Fig. S1), with Mueller matrix $\mathbf{M}_{HW\_TA}$ is used for the correction of the effect of this rotation on

$I_{LA\_TA\_s}$ (Section 4.1 in manuscript).

$$\frac{I_{LA\_TA\_s}}{\eta_{s\_TA}E_{LA\_TA}} = \boldsymbol{e}\mathbf{M}_{s\_TA}\mathbf{M}_{HW\_TA}\mathbf{M}_{O\_TA}\mathbf{R}_{TA}[\mathbf{F}+\mathbf{G}]\boldsymbol{i}_{LA} =$$

$$= \begin{bmatrix}1 & 0 & 0 & 0\end{bmatrix} T_{s\_TA} \begin{bmatrix}1 & D_{s\_TA} & 0 & 0\\ D_{s\_TA} & 1 & 0 & 0\\ 0 & 0 & 0 & 0\\ 0 & 0 & 0 & 0\end{bmatrix} \begin{bmatrix}1 & 0 & 0 & 0\\ 0 & c_{4\theta_{TA}} & s_{4\theta_{TA}} & 0\\ 0 & s_{4\theta_{TA}} & -c_{4\theta_{TA}} & 0\\ 0 & 0 & 0 & -1\end{bmatrix} \cdot$$

$$\cdot T_{O\_TA} \begin{bmatrix}1 & 0 & 0 & 0\\ 0 & 1 & 0 & 0\\ 0 & 0 & 1 & 0\\ 0 & 0 & 0 & 1\end{bmatrix} \begin{bmatrix}1 & 0 & 0 & 0\\ 0 & c_{2\omega_{TA}} & s_{2\omega_{TA}} & 0\\ 0 & -s_{2\omega_{TA}} & c_{2\omega_{TA}} & 0\\ 0 & 0 & 0 & 1\end{bmatrix} \cdot$$

$$\cdot F_{11} \begin{bmatrix}f_{11}+g_{11} & f_{12} & f_{13} & f_{14}\\ f_{12} & f_{22}+g_{22} & f_{23} & f_{24}\\ -f_{13} & -f_{23} & f_{33}+g_{33} & f_{34}\\ f_{14} & f_{24} & -f_{34} & f_{44}+g_{44}\end{bmatrix} \begin{bmatrix}1\\ c_{4\vartheta_{LA}}\\ s_{4\vartheta_{LA}}\\ 0\end{bmatrix} \Rightarrow$$

$$\Rightarrow \frac{I_{LA\_TA\_s}}{\eta_{s\_TA}E_{LA\_TA}T_{s\_TA}T_{O\_TA}F_{11}} = \Big[f_{11}+g_{11}+c_{4\vartheta_{LA}}f_{12}+s_{4\vartheta_{LA}}f_{13}+$$
$$+ D_{s\_TA}c_{(4\theta_{TA}+2\omega_{TA})}[f_{12}+c_{4\vartheta_{LA}}(f_{22}+g_{22})+s_{4\vartheta_{LA}}f_{23}]+$$
$$+ D_{s\_TA}s_{(4\theta_{TA}+2\omega_{TA})}[-f_{13}-c_{4\vartheta_{LA}}f_{23}+s_{4\vartheta_{LA}}(f_{33}+g_{33})]\Big] \quad \text{(S16)}$$

After correcting the effect due to the rotation of the detection unit after telescope A, by setting the fast-axis-angle of HWP_{TA} at $\theta_{TA} = -\frac{\omega_{TA}}{2}$ (Section 4.1 in manuscript), Eq. S16 is written as Eq. S17.

$$\frac{I_{LA\_TA\_s(\theta_{TA}=-\frac{\omega_{TA}}{2})}}{\eta_{s\_TA}E_{LA\_TA}T_{s\_TA}T_{O\_TA}F_{11}} = f_{11}+g_{11}+c_{4\vartheta_{LA}}f_{12}+s_{4\vartheta_{LA}}f_{13}+$$
$$+ D_{s\_TA}(f_{12}+c_{4\vartheta_{LA}}(f_{22}+g_{22})+s_{4\vartheta_{LA}}f_{23}) \quad \text{(S17)}$$

S2.3 $\mathbf{I_{LB\_TA\_s}}$: The signals from laser B, at the detection unit after telescope A

The measurements of the backscatterred light of laser B at the detectors of telescope A are provided in Eq. S18. The HWP_{TA} (Fig. S1), with Mueller matrix $\mathbf{M}_{HW\_TA}$ is used for the correction of the effect of the rotation of the detection unit after telescope A, on $I_{LB\_TA\_s}$ (Section 4.1 in manuscript).

$$\frac{I_{LB\_TA\_s}}{\eta_{s\_TA}E_{LB\_TA}} = \boldsymbol{e}\mathbf{M}_{s\_TA}\mathbf{M}_{HW\_TA}\mathbf{M}_{O\_TA}\mathbf{R}_{TA}[\mathbf{F}+\mathbf{G}]\boldsymbol{i}_{LB} =$$

$$= \begin{bmatrix}1 & 0 & 0 & 0\end{bmatrix} T_{s\_TA} \begin{bmatrix}1 & D_{s\_TA} & 0 & 0\\ D_{s\_TA} & 1 & 0 & 0\\ 0 & 0 & 0 & 0\\ 0 & 0 & 0 & 0\end{bmatrix} \begin{bmatrix}1 & 0 & 0 & 0\\ 0 & c_{4\theta_{TA}} & s_{4\theta_{TA}} & 0\\ 0 & s_{4\theta_{TA}} & -c_{4\theta_{TA}} & 0\\ 0 & 0 & 0 & -1\end{bmatrix} \cdot$$

$$\cdot\, T_{O\_TA} \begin{bmatrix}1 & 0 & 0 & 0\\ 0 & 1 & 0 & 0\\ 0 & 0 & 1 & 0\\ 0 & 0 & 0 & 1\end{bmatrix} \begin{bmatrix}1 & 0 & 0 & 0\\ 0 & c_{2\omega_{TA}} & s_{2\omega_{TA}} & 0\\ 0 & -s_{2\omega_{TA}} & c_{2\omega_{TA}} & 0\\ 0 & 0 & 0 & 1\end{bmatrix} \cdot$$

$$\cdot\, F_{11} \begin{bmatrix}f_{11}+g_{11} & f_{12} & f_{13} & f_{14}\\ f_{12} & f_{22}+g_{22} & f_{23} & f_{24}\\ -f_{13} & -f_{23} & f_{33}+g_{33} & f_{34}\\ f_{14} & f_{24} & -f_{34} & f_{44}+g_{44}\end{bmatrix} \begin{bmatrix}1\\ c_{2\varphi_{LB}}c_{(4\theta_{LB}-2\phi_{LB})}\\ c_{2\varphi_{LB}}s_{(4\theta_{LB}-2\phi_{LB})}\\ -s_{2\varphi_{LB}}\end{bmatrix} \Rightarrow$$

$$\begin{aligned}\Rightarrow \frac{I_{LB\_TA\_s}}{\eta_{s\_TA}E_{LB\_TA}T_{s\_TA}T_{O\_TA}F_{11}} = {} & f_{11} + [D_{s\_TA}c_{(4\theta_{TA}+2\omega_{TA})} + c_{2\varphi_{LB}}c_{(4\theta_{LB}-2\phi_{LB})}]f_{12} + \\ & + [c_{2\varphi_{LB}}s_{(4\theta_{LB}-2\phi_{LB})} - D_{s\_TA}s_{(4\theta_{TA}+2\omega_{TA})}]f_{13} \\ & - s_{2\varphi_{LB}}f_{14} + D_{s\_TA}c_{(4\theta_{TA}+2\omega_{TA})}c_{2\varphi_{LB}}c_{(4\theta_{LB}-2\phi_{LB})}f_{22} + \\ & + D_{s\_TA}c_{2\varphi_{LB}}\Big[c_{(4\theta_{TA}+2\omega_{TA})}s_{(4\theta_{LB}-2\phi_{LB})} - s_{(4\theta_{TA}+2\omega_{TA})}c_{(4\theta_{LB}-2\phi_{LB})}\Big]f_{23} + \\ & - D_{s\_TA}c_{(4\theta_{TA}+2\omega_{TA})}s_{2\varphi_{LB}}f_{24} + \\ & + D_{s\_TA}s_{(4\theta_{TA}+2\omega_{TA})}c_{2\varphi_{LB}}s_{(4\theta_{LB}-2\phi_{LB})}f_{33} + \\ & - D_{s\_TA}s_{(4\theta_{TA}+2\omega_{TA})}s_{2\varphi_{LB}}f_{34} + \\ & + g_{11} + D_{s\_TA}c_{(4\theta_{TA}+2\omega_{TA})}c_{2\varphi_{LB}}c_{(4\theta_{LB}-2\phi_{LB})}g_{22} + \\ & + D_{s\_TA}s_{(4\theta_{TA}+2\omega_{TA})}c_{2\varphi_{LB}}s_{(4\theta_{LB}-2\phi_{LB})}g_{33}\end{aligned} \tag{S18}$$

After correcting for the rotation of the detection unit after telescope A, by setting the fast-axis-angle of HWP_{TA} at $\theta_{TA} = -\frac{\omega_{TA}}{2}$ (Section 4.1 in manuscript), Eq. S18 is written as Eq. S19.

$$\begin{aligned}\frac{I_{LB\_TA\_s(\theta_{TA}=-\frac{\omega_{TA}}{2})}}{\eta_{s\_TA}E_{LB\_TA}T_{s\_TA}T_{O\_TA}F_{11}} = {} & f_{11} + [D_{s\_TA} + c_{2\varphi_{LB}}c_{(4\theta_{LB}-2\phi_{LB})}]f_{12} + c_{2\varphi_{LB}}s_{(4\theta_{LB}-2\phi_{LB})}f_{13} + \\ & - s_{2\phi_{LB}}f_{14} + D_{s\_TA}c_{2\varphi_{LB}}c_{(4\theta_{LB}-2\phi_{LB})}f_{22} + D_{s\_TA}c_{2\varphi_{LB}}s_{(4\theta_{LB}-2\phi_{LB})}f_{23} + \\ & - D_{s\_TA}s_{2\varphi_{LB}}f_{24} + g_{11} + D_{s\_TA}c_{2\varphi_{LB}}c_{(4\theta_{LB}-2\phi_{LB})}g_{22}\end{aligned} \tag{S19}$$

S2.4 $\mathbf{I_{LA\_TB\_s}}$: The signals from laser A, at the detection unit after telescope B

The measurements of the backscatterred light of laser A at the detectors of telescope B are provided in Eq. S21. The rotation of the detection unit after telescope B by an angle ω_{TB} (Fig.

S2) is taken into account using the rotation matrix $\mathbf{R}_{TB}(-\omega_{TB})$, and as shown in Eq. S21 it does not affect the measurements.
The HWP_{TB} (Fig. S1), with Mueller matrix $\mathbf{M}_{HW\_TB}$ is used for checking that the QWP_{TB} is at 45^o with respect of the $x_{DU_{TB}}$-axis (Fig. S2), as shown in Section S4. The Mueller matrix of the QWP_{TB} with $\phi_{TB} = 45^o$ is provided in Eq. S20.

$$\mathbf{M}_{QW\_TB(\phi_{TB}=45^o)} = \begin{bmatrix} 1 & 0 & 0 & 0 \\ 0 & c_{90}^2 & s_{90}c_{90} & -s_{90} \\ 0 & s_{90}c_{90} & s_{90}^2 & c_{90} \\ 0 & s_{90} & -c_{90} & 0 \end{bmatrix} = \begin{bmatrix} 1 & 0 & 0 & 0 \\ 0 & 0 & 0 & -1 \\ 0 & 0 & 1 & 0 \\ 0 & 1 & 0 & 0 \end{bmatrix} \tag{S20}$$

$$\begin{aligned} \frac{I_{LA\_TB\_s}}{\eta_{s\_TB}E_{LA\_TB}} &= \boldsymbol{e}\mathbf{M}_{s\_TB}\mathbf{M}_{QW\_TB}\mathbf{M}_{HW\_TB}\mathbf{M}_{O\_TB}\mathbf{R}_{TB}[\mathbf{F}+\mathbf{G}]\boldsymbol{i}_{LA} = \\ &= \begin{bmatrix} 1 & 0 & 0 & 0 \end{bmatrix} T_{s\_TB} \begin{bmatrix} 1 & D_{s\_TB} & 0 & 0 \\ D_{s\_TB} & 1 & 0 & 0 \\ 0 & 0 & 0 & 0 \\ 0 & 0 & 0 & 0 \end{bmatrix} \begin{bmatrix} 1 & 0 & 0 & 0 \\ 0 & 0 & 0 & -1 \\ 0 & 0 & 1 & 0 \\ 0 & 1 & 0 & 0 \end{bmatrix} \begin{bmatrix} 1 & 0 & 0 & 0 \\ 0 & c_{4\theta_{TB}} & s_{4\theta_{TB}} & 0 \\ 0 & s_{4\theta_{TB}} & -c_{4\theta_{TB}} & 0 \\ 0 & 0 & 0 & -1 \end{bmatrix} \cdot \\ &\cdot T_{O\_TB} \begin{bmatrix} 1 & 0 & 0 & 0 \\ 0 & 1 & 0 & 0 \\ 0 & 0 & 1 & 0 \\ 0 & 0 & 0 & 1 \end{bmatrix} \begin{bmatrix} 1 & 0 & 0 & 0 \\ 0 & c_{2\omega_{TB}} & s_{2\omega_{TB}} & 0 \\ 0 & -s_{2\omega_{TB}} & c_{2\omega_{TB}} & 0 \\ 0 & 0 & 0 & 1 \end{bmatrix} \cdot \\ &\cdot F_{11} \begin{bmatrix} f_{11}+g_{11} & f_{12} & f_{13} & f_{14} \\ f_{12} & f_{22}+g_{22} & f_{23} & f_{24} \\ -f_{13} & -f_{23} & f_{33}+g_{33} & f_{34} \\ f_{14} & f_{24} & -f_{34} & f_{44}+g_{44} \end{bmatrix} \begin{bmatrix} 1 \\ c_{4\vartheta_{LA}} \\ s_{4\vartheta_{LA}} \\ 0 \end{bmatrix} \Rightarrow \end{aligned}$$

$$\begin{aligned} \Rightarrow \frac{I_{LA\_TB\_s}}{\eta_{s\_TB}E_{LA\_TB}T_{s\_TB}T_{O\_TB}F_{11}} &= f_{11} + c_{4\vartheta_{LA}}f_{12} + s_{4\vartheta_{LA}}f_{13} + D_{s\_TB}f_{14} + D_{s\_TB}c_{4\vartheta_{LA}}f_{24} + \\ &- D_{s\_TB}s_{4\vartheta_{LA}}f_{34} + g_{11} \end{aligned} \tag{S21}$$

S2.5 $\mathbf{I_{LB\_TB\_s}}$: The signals from laser B, at the detection unit after telescope B

The measurements of the backscatterred light of laser B at the detection unit after telescope B are provided in Eq. S22.

$$\frac{I_{LB\_TB\_s}}{\eta_{s\_TB}E_{LB\_TB}} = \boldsymbol{e}\mathbf{M}_{s\_TB}\mathbf{M}_{QW\_TB}\mathbf{M}_{HW\_TB}\mathbf{M}_{O\_TB}\mathbf{R}_{TB}[\mathbf{F}+\mathbf{G}]\boldsymbol{i}_{LB} =$$

$$= \begin{bmatrix}1 & 0 & 0 & 0\end{bmatrix} T_{s\_TB} \begin{bmatrix}1 & D_{s\_TB} & 0 & 0\\ D_{s\_TB} & 1 & 0 & 0\\ 0 & 0 & 0 & 0\\ 0 & 0 & 0 & 0\end{bmatrix} \begin{bmatrix}1 & 0 & 0 & 0\\ 0 & 0 & 0 & -1\\ 0 & 0 & 1 & 0\\ 0 & 1 & 0 & 0\end{bmatrix} \begin{bmatrix}1 & 0 & 0 & 0\\ 0 & c_{4\theta_{TB}} & s_{4\theta_{TB}} & 0\\ 0 & s_{4\theta_{TB}} & -c_{4\theta_{TB}} & 0\\ 0 & 0 & 0 & -1\end{bmatrix} \cdot$$

$$\cdot T_{O\_TB} \begin{bmatrix}1 & 0 & 0 & 0\\ 0 & 1 & 0 & 0\\ 0 & 0 & 1 & 0\\ 0 & 0 & 0 & 1\end{bmatrix} \begin{bmatrix}1 & 0 & 0 & 0\\ 0 & c_{2\omega_{TB}} & s_{2\omega_{TB}} & 0\\ 0 & -s_{2\omega_{TB}} & c_{2\omega_{TB}} & 0\\ 0 & 0 & 0 & 1\end{bmatrix} \cdot$$

$$\cdot F_{11} \begin{bmatrix}f_{11}+g_{11} & f_{12} & f_{13} & f_{14}\\ f_{12} & f_{22}+g_{22} & f_{23} & f_{24}\\ -f_{13} & -f_{23} & f_{33}+g_{33} & f_{34}\\ f_{14} & f_{24} & -f_{34} & f_{44}+g_{44}\end{bmatrix} \begin{bmatrix}1\\ c_{2\varphi_{LB}}c_{(4\theta_{LB}-2\phi_{LB})}\\ c_{2\varphi_{LB}}s_{(4\theta_{LB}-2\phi_{LB})}\\ -s_{2\varphi_{LB}}\end{bmatrix} \Rightarrow$$

$$\Rightarrow \frac{I_{LB\_TB\_s}}{\eta_{s\_TB}E_{LB\_TB}T_{s\_TB}T_{O\_TB}F_{11}} = f_{11} + c_{2\varphi_{LB}}c_{(4\theta_{LB}-2\phi_{LB})}f_{12} + c_{2\varphi_{LB}}s_{(4\theta_{LB}-2\phi_{LB})}f_{13} +$$
$$+ (D_{s\_TB} - s_{2\varphi_{LB}})f_{14} + D_{s\_TB}c_{2\varphi_{LB}}c_{(4\theta_{LB}-2\phi_{LB})}f_{24} +$$
$$- D_{s\_TB}c_{2\varphi_{LB}}s_{(4\theta_{LB}-2\phi_{LB})}f_{34} - D_{s\_TB}s_{2\varphi_{LB}}f_{44} +$$
$$+ g_{11} - D_{s\_TB}s_{2\varphi_{LB}}g_{44} \quad \text{(S22)}$$

S3 Calculation of the measured intensities after we place a linear polarizer at 45° in front of the emission unit of laser A

After placing a linear polarizer in front of the window in front of the emission unit of laser A, at 45^o from x_F-axis (Fig. S3), the Stokes vector of the emitted light $\boldsymbol{i}_{LA\_45^o}$ is provided by Eq. S23. The measured intensities $I_{LA\_TA\_s\_45^o}$ at the detectors after telescope A are provided in Eq. S24.
In Eq. S23 we consider an ideal linear polarizer. The Mueller matrix of the ideal linear polarizer at 45^o ($\mathbf{LP}_{45^o}$) is taken from the Handbook of optics (Table 1 in section 14.11). In Eq. S24 we consider randomly-oriented particles.

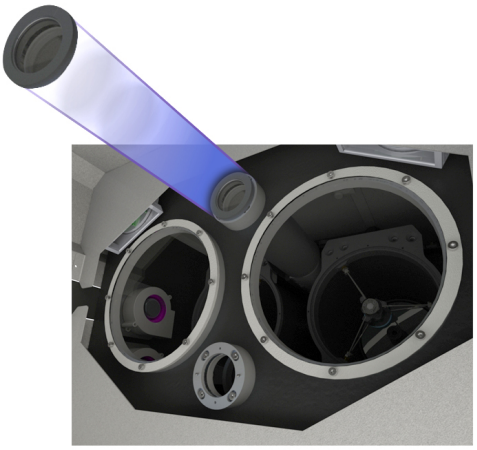

Figure S3: Linear polarizer in front of the window of laser A, placed at 45^o from x_F-axis.

$$\boldsymbol{i}_{LA\_45^o} = \mathbf{LP}_{45^o}\boldsymbol{i}_{LA} = \frac{1}{2}\begin{bmatrix}1 & 0 & 1 & 0\\ 0 & 0 & 0 & 0\\ 1 & 0 & 1 & 0\\ 0 & 0 & 0 & 0\end{bmatrix}\begin{bmatrix}1\\ c_{4\vartheta_{LA}}\\ s_{4\vartheta_{LA}}\\ 0\end{bmatrix} = \frac{1+s_{4\vartheta_{LA}}}{2}\begin{bmatrix}1\\ 0\\ 1\\ 0\end{bmatrix} \tag{S23}$$

$$\frac{I_{LA\_TA\_s\_45^o}}{\eta_{s\_TA}E_{LA\_TA}} = \boldsymbol{e}\mathbf{M}_{s\_TA}\mathbf{M}_{HW\_TA}\mathbf{M}_{O\_TA}\mathbf{R}_{TA}[\mathbf{F}+\mathbf{G}]\boldsymbol{i}_{LA\_45^o} =$$

$$= \begin{bmatrix}1 & 0 & 0 & 0\end{bmatrix} T_{s\_TA} \begin{bmatrix}1 & D_{s\_TA} & 0 & 0\\ D_{s\_TA} & 1 & 0 & 0\\ 0 & 0 & 0 & 0\\ 0 & 0 & 0 & 0\end{bmatrix} \begin{bmatrix}1 & 0 & 0 & 0\\ 0 & c_{4\theta_{TA}} & s_{4\theta_{TA}} & 0\\ 0 & s_{4\theta_{TA}} & -c_{4\theta_{TA}} & 0\\ 0 & 0 & 0 & -1\end{bmatrix} \cdot$$

$$\cdot T_{O\_TA} \begin{bmatrix}1 & 0 & 0 & 0\\ 0 & 1 & 0 & 0\\ 0 & 0 & 1 & 0\\ 0 & 0 & 0 & 1\end{bmatrix} \begin{bmatrix}1 & 0 & 0 & 0\\ 0 & c_{2\omega_{TA}} & s_{2\omega_{TA}} & 0\\ 0 & -s_{2\omega_{TA}} & c_{2\omega_{TA}} & 0\\ 0 & 0 & 0 & 1\end{bmatrix} \cdot$$

$$\cdot F_{11} \begin{bmatrix}f_{11}+g_{11} & 0 & 0 & 0\\ 0 & f_{22}+g_{22} & 0 & 0\\ 0 & 0 & f_{33}+g_{33} & 0\\ 0 & 0 & 0 & f_{44}+g_{44}\end{bmatrix} \frac{1+s_{4\vartheta_{LA}}}{2} \begin{bmatrix}1\\0\\1\\0\end{bmatrix} \Rightarrow$$

$$\Rightarrow \frac{I_{LA\_TA\_s\_45^o}}{\eta_{s\_TA}E_{LA\_TA}T_{s\_TA}T_{O\_TA}F_{11}} = \frac{1}{2}\Big[f_{11}+g_{11}+D_{s\_TA}s_{(4\theta_{TA}+2\omega_{TA})}(f_{33}+g_{33})\Big](1+s_{4\vartheta_{LA}}) \tag{S24}$$

S4 Check that the fast-axis-angle of $\mathbf{QWP_{TB}}$ is at 45° with respect to $\mathbf{x_{DU_{TB}}}$-axis

In order to check for the accurate placement of the fast-axis-angle of QWP_{TB} at 45^o with respect to the $x_{DU_{TB}}$-axis, we rotate the HWP_{TB} before QWP_{TB}, at various random positions. If $I_{LA\_TB\_s}$ changes when HWP_{TB} is placed at the different positions, the QWP_{TB} is not placed at 45^o with respect to the $x_{DU_{TB}}$-axis.

Considering a misalignment of QWP_{TB} by ε_{TB}, the fast-axis-angle of QWP_{TB} is $\phi_{TB} = 45^o + \varepsilon_{TB}$ and the measurements at the detection unit after telescope B ($I_{LA\_TB\_s\_(\phi_{TB}=45^o+\varepsilon_{TB})}$) change with the rotation of the HWP_{TB}, as shown in Eq. S26. If $\varepsilon_{TB} = 0$,then $\phi_{TB} = 45^o$, and the measurements $I_{LA\_TB\_s\_(\phi_{TB}=45^o)}$, do not change with the rotation of the HWP_{TB} (Eq. S27). The same is true for $I_{LB\_TB\_s}$ (not shown here).

$$\mathbf{M}_{QW\_TB\_(\phi_{TB}=45^o+\varepsilon_{TB})} = \begin{bmatrix} 1 & 0 & 0 & 0 \\ 0 & c^2_{2(45+\varepsilon_{TB})} & s_{2(45+\varepsilon_{TB})}c_{2(45+\varepsilon_{TB})} & -s_{2(45+\varepsilon_{TB})} \\ 0 & s_{2(45+\varepsilon_{TB})}c_{2(45+\varepsilon_{TB})} & s^2_{2(45+\varepsilon_{TB})} & c_{2(45+\varepsilon_{TB})} \\ 0 & s_{2(45+\varepsilon_{TB})} & -c_{2(45+\varepsilon_{TB})} & 0 \end{bmatrix} = \tag{S25}$$
$$= \begin{bmatrix} 1 & 0 & 0 & 0 \\ 0 & s^2_{2\varepsilon_{TB}} & -s_{2\varepsilon_{TB}}c_{2\varepsilon_{TB}} & -c_{2\varepsilon_{TB}} \\ 0 & -s_{2\varepsilon_{TB}}c_{2\varepsilon_{TB}} & c^2_{2\varepsilon_{TB}} & -s_{2\varepsilon_{TB}} \\ 0 & c_{2\varepsilon_{TB}} & s_{2\varepsilon_{TB}} & 0 \end{bmatrix}$$

$$\frac{I_{LA\_TB\_s\_(\phi_{TB}=45^o+\varepsilon_{TB})}}{\eta_{s\_TB}E_{LA\_TB}} = \boldsymbol{e}\mathbf{M}_{s\_TB}\mathbf{M}_{QW\_TB\_(\phi_{TB}=45^o+\varepsilon_{TB})}\mathbf{M}_{HW\_TB}\mathbf{M}_{O\_TB}\mathbf{R}_{TB}[\mathbf{F}+\mathbf{G}]\boldsymbol{i}_{LA} =$$
$$= \begin{bmatrix} 1 & 0 & 0 & 0 \end{bmatrix} T_{s\_TB} \begin{bmatrix} 1 & D_{s\_TB} & 0 & 0 \\ D_{s\_TB} & 1 & 0 & 0 \\ 0 & 0 & 0 & 0 \\ 0 & 0 & 0 & 0 \end{bmatrix} \cdot$$
$$\cdot \begin{bmatrix} 1 & 0 & 0 & 0 \\ 0 & s^2_{2\varepsilon_{TB}} & -s_{2\varepsilon_{TB}}c_{2\varepsilon_{TB}} & -c_{2\varepsilon_{TB}} \\ 0 & -s_{2\varepsilon_{TB}}c_{2\varepsilon_{TB}} & c^2_{2\varepsilon_{TB}} & -s_{2\varepsilon_{TB}} \\ 0 & c_{2\varepsilon_{TB}} & s_{2\varepsilon_{TB}} & 0 \end{bmatrix} \begin{bmatrix} 1 & 0 & 0 & 0 \\ 0 & c_{4\theta_{TB}} & s_{4\theta_{TB}} & 0 \\ 0 & s_{4\theta_{TB}} & -c_{4\theta_{TB}} & 0 \\ 0 & 0 & 0 & -1 \end{bmatrix} \cdot$$
$$\cdot T_{O\_TB} \begin{bmatrix} 1 & 0 & 0 & 0 \\ 0 & 1 & 0 & 0 \\ 0 & 0 & 1 & 0 \\ 0 & 0 & 0 & 1 \end{bmatrix} \begin{bmatrix} 1 & 0 & 0 & 0 \\ 0 & c_{2\omega_{TB}} & s_{2\omega_{TB}} & 0 \\ 0 & -s_{2\omega_{TB}} & c_{2\omega_{TB}} & 0 \\ 0 & 0 & 0 & 1 \end{bmatrix} \cdot$$
$$\cdot F_{11} \begin{bmatrix} f_{11}+g_{11} & f_{12} & f_{13} & f_{14} \\ f_{12} & f_{22}+g_{22} & f_{23} & f_{24} \\ -f_{13} & -f_{23} & f_{33}+g_{33} & f_{34} \\ f_{14} & f_{24} & -f_{34} & f_{44}+g_{44} \end{bmatrix} \begin{bmatrix} 1 \\ 0 \\ 1 \\ 0 \end{bmatrix} \Rightarrow$$

$$\Rightarrow \frac{I_{LA\_TB\_s\_(\phi_{TB}=45^o+\varepsilon_{TB})}}{\eta_{s\_TB}E_{LA\_TB}T_{s\_TB}T_{O\_TB}F_{11}} = f_{11} + g_{11} + f_{13} + D_{s\_TB}c_{2\varepsilon_{TB}}f_{14} - D_{s\_TB}c_{2\varepsilon_{TB}}f_{34} + \\ + D_{s\_TB}s^2_{2\varepsilon_{TB}}[c_{(4\theta_{TB}+2\omega_{TB})}(f_{12}+f_{23}) + \\ + s_{(4\theta_{TB}+2\omega_{TB})}(-f_{13}+f_{33}+g_{33})] + \\ - D_{s\_TB}c_{2\varepsilon_{TB}}s_{2\varepsilon_{TB}}[s_{(4\theta_{TB}+2\omega_{TB})}(f_{12}+f_{23}) + \\ - c_{(4\theta_{TB}+2\omega_{TB})}(-f_{13}+f_{33}+g_{33})] \tag{S26}$$

$$\frac{I_{LA\_TB\_s\_(\phi_{TB}=45^o)}}{\eta_{s\_TB}E_{LA\_TB}T_{s\_TB}T_{O\_TB}F_{11}} = f_{11} + f_{13} + D_{s\_TB}f_{14} - D_{s\_TB}f_{34} + g_{11} \tag{S27}$$

S5 References

Freudenthaler, V.: About the effects of polarising optics on lidar signals and the Δ90-calibration, Atmos. Meas. Tech., 9, 4181-4255, 2016a, doi: 10.5194/amt-9-4181-2016
Handbook of Optics, Volume I - Geometrical and Physical Optics, Polarized Light, Components and Instruments (3rd Edition), Bass, M. (Ed.). McGraw Hill Professional, 2009.

S6 Acronyms and symbols

In the following table a list of acronyms and symbols is provided. In the third column we provide the equation where we first find them.

a	The polarization parameter of the atmosphere	
α	The angle of the polarization ellipse	
A_k	Area of telescope k	Eq. S11
b	The degree of linear polarization	
c_x	cosine of x	Eq. S3
δ	volume linear depolarization ratio (VLDR)	
Δ_R	The retardance of $\mathbf{M}_R$	Eq. S9
Δ_T	The retardance of $\mathbf{M}_T$	Eq. S7
Δ_{T_O}	The retardance of $\mathbf{M}_O$	Eq. S3
D_O	The diattenuation parameter of $\mathbf{M}_O$	Eq. S3
D_R	The diattenuation parameter of $\mathbf{M}_R$	Eq. S9
D_T	The diattenuation parameter of $\mathbf{M}_T$	Eq. S7
DU_k	The coordinate system of the detection unit after telescope k	
$\boldsymbol{e}$	$[1,0,0,0]$	Eq. S11
E_{oi}	The pulse energy of the laser i	Eq. S11
E_{i_k}	$E_{i\_k} = A_k O_{i\_k} T(0,r)^{-2} E_{oi}$	
$\mathbf{F}$	The backscatter Stokes phase matrix of the aerosol particles in the atmosphere	Eq. S1
$\boldsymbol{f}$	The vectorized matrix $\mathbf{F}$, $f_{m+4(n-1)} = F_{mn}$	
f_{ij}	$f_{ij} = \frac{F_{ij}}{F_{11}}$	
F_{LA_k}	The orientation flag measured with laser A at telescope k	
$\mathbf{G}$	The backscatter Stokes phase matrix of the the gases in the atmosphere	Eq. S2
$\boldsymbol{g}$	The vectorized matrix $\mathbf{G}$, $g_{m+4(n-1)} = G_{mn}$	
g_{ij}	$g_{ij} = \frac{G_{ij}}{F_{11}}$	
HWP	Half Wave Plate	Eq. S5
i	Laser $i = LA, LB$	Eq. S11
$\boldsymbol{i}_i$	The Stokes vector of light from the emission unit of laser i	Eq. S11
$\boldsymbol{i}_g$	The Stokes vector of the background skylight	
$\boldsymbol{i}_{LA\_45^o}$	The Stokes vector of light from the emission unit of laser A, after placing a LP in front of the window in front of the emission unit, at 45^o from x_F-axis	Eq. S23
$\boldsymbol{i}_{lsr\_i}$	The Stokes vector of the light emitted directly from laser i	

$I^*_{i\_k\_s}$	The signal from laser i at the detector $s = T$ or R after telescope k, including the background skylight and the electronic noise at the detectors	
$I_{i\_k\_s}$	The signal from laser i at the detector $s = T$ or R after telescope k	Eq. S11
$I_{i\_TA\_s(\theta_{TA}=-\frac{\omega_{TA}}{2})}$	The signal from laser i at the detector $s = T$ or R after telescope A, after correcting for the effect of the rotation of the detection unit, by setting the HWP_{TA} at $\theta_{TA} = -\frac{\omega_{TA}}{2}$	Eq. S19
$I_{LA\_k\_s\_45^o}$	The signal from laser A at the detector $s = T$ or R after telescope k, after placing a LP in front of the window in front of the emission unit of laser A, at 45^o from x_F-axis	Eq. S24
$I_{i\_TB\_s(\phi_{TB}=45^o+\varepsilon_{TB})}$	The signal $I_{i\_TB\_s}$, in case the fast-axis-angle of QWP_{TB} is misaligned by ε_{TB} ($\phi_{TB} = 45^o + \varepsilon_{TB}$)	Eq. S26
k	Telescope $k = TA, TB$	Eq. S11
η_k	The calibration factor of the ratio of the intensities at the detectors R and T after telescope k	
η_{s_k}	The amplification of the signal at the detector $s = R$ or T after telescope k	
θ	The fast-axis-angle of the HWP	Eq. S5
ϑ_{LA}	$\vartheta_{LA} = \theta_{LA} - \frac{\alpha_{LA}}{2}$, where θ_{LA} is the fast-axis-angle of the HWP_{LA} and α_{LA} is the angle of the polarization ellipse of the light emitted directly from laser A	Eq. S14
$\mathbf{M}_{HW}$	Mueller matrix of the HWP	Eq. S5
$\boldsymbol{M}_{i\_k}$	The row vector expressing the measured polarization at the detection unit after telescope k	
$\mathbf{M}_O$	Mueller matrix of the receiver optics (i.e. telescope k, collimating lenses, bandpass filter)	Eq. S3
$\mathbf{M_T}$	Mueller matrix of the transmitting part of the PBS, followed by cleaning polarizers	Eq. S8
$\mathbf{M_R}$	Mueller matrix of the reflecting part of the PBS, followed by cleaning polarizers	Eq. S10
$\mathbf{M}_{QW}$	Mueller matrix of the QWP	Eq. S6
$\mathbf{M}_{QW\_TB(\phi_{TB}=45^o)}$	Mueller matrix of the QWP_{TB} with its fast-axis-angle at $\phi_{TB} = 45^o$, with respect to the reference coordinate system	Eq. S20
O_{i_k}	The laser beam receiver field-of-view overlap function, for laser i and telescope k	Eq. S11
$\boldsymbol{p}_{i\_k}$	$p_{i\_k_{m+4(n-1)}} = M_{i\_k_m} i_{i_n}$	
PBS	Polarizing Beam Splitter	
QWP	Quarter Wave Plate	
$\mathbf{R}_k$	The rotation matrix used to describe the rotation of the detection unit after telescope k, with respect to the frame coordinate system	Eq. S16

s	$s = T, R$, the "Transmitted" and "Reflected" channels after the PBS	
s_x	sine of x	
$T(0, r)$	The transmission of the atmosphere between the lidar at range $r = 0$ and a specific range r in the atmosphere	Eq. S11
T_O	The transmittance of $\mathbf{M}_O$	Eq. S3
T_R	The reflectance of $\mathbf{M}_R$	Eq. S9
T_T	The transmittance of $\mathbf{M}_T$	Eq. S7
VLDR	Volume Linear Depolarization Ratio	
Z_O	The retardation parameter of $\mathbf{M}_O$	Eq. S3
Z_R	The retardation parameter of $\mathbf{M}_R$	Eq. S9
Z_T	The retardation parameter of $\mathbf{M}_T$	Eq. S7
ϕ	The fast-axis-angle of QWP	Eq. S6
φ_{LB}	$\varphi_{LB} = \phi_{LB} - \alpha_{LB}$, where ϕ_{LB} is the fast-axis-angle of the QWP_{LB} and α_{LB} is the angle of the polarization ellipse of the light emitted directly from laser B	Eq. S15
ω_k	The rotation angle of the detection unit after telescope k, with respect to the frame coordinate system	Eq. S16
x_F, y_F, z_F	The axes of the frame coordinate system (used as the reference coordinate system)	
x_{DU_k}, y_{DU_k}, z_{DU_k}	The axes of the DU_k coordinate system	
$y_{N_{i\_k\_s}}$	The electronic background of the $s = T$ or R detector at the detection unit after telescope k, for detecting the backscattered signal of laser i	